# SURFACE ENHANCED RAMAN SPECTROSCOPY: A METROLOGICAL TOOL FOR FUNGICIDE DETECTION

*Luisa Mandrile*[1], Andrea Giovannozzi[2], Francesca Durbiano[2], *Andrea Mario Rossi*[2]
[1] Unito (Faculty of chemistry), Turin, Italy, l.mandrile@inrim.it
[2] INRIM (Quality of life division), Turin, Italy, a.rossi@inrim.it

***Abstract*** – The scope of this work is to standardize a Surface Enhanced Raman Scattering methodology for the detection of food contaminants in order to provide good compromise between sensitivity and reproducibility of analysis. A stable methodology to analyse fungicide's traces directly on fruit peal by depositing gold nanoparticles on its surface is proposed. Different types of AuNPs for SERS where synthetized and tested. A comparative study between different AuNPs was performed in order to maximize the enhancement factor. Sensitive and specific method for *in-situ* detection is provided and two different strategies for quantification are proposed. A standardized method based on SERS technology for the analysis of fungicide traces on an apple's peal was set and validated.

***Keywords***: Raman mapping, Surface Enhanced Raman Scattering, Gold Nanoparticles, Fungicide.

## 1. INTRODUCTION

In the last decades, Surface-Enhanced Raman Scattering (SERS) has become a mature vibrational spectroscopic technique and the number of applications in the chemical, material, and life sciences has rapidly increased [1]. In comparison with the most diffused techniques such as high performance liquid chromatography (HPLC) and mass-spectrometry, Raman spectroscopy allows fast detection times, high selectivity due to the Raman fingerprint of molecules without any preliminary treatment of the sample. Moreover, the sensitivity of the traditional Raman technique can be increased of several orders of magnitude in SERS technique due to the enhancement of the Raman scattering of molecules absorbed onto, or microscopically close to, a suitable plasmonically active surface, such as roughened nanostructured metal surface, or metal colloids [2]. For all these reasons SERS represents a good candidate for food control analysis. Nevertheless, standardized methods of production and application of SERS systems are still needed in order to provide good compromise between sensitivity and reproducibility of analysis [3].

For this study pyrimethanil (PMT) fungicide was chosen as a representative test material. It is a widely used fungicide and, although it does not present toxicity to humans, it is a very harmful substance, especially to aquatic environments and, as a pesticide, in 2007 it has been included in Annex I COUNCIL DIRECTIVE (91/414 / EEC) concerning plant protection products. Pyrimethanil is employed on several horticultural species with declared maximum residue level established by EFSA report (7 ppm for pome fruits) [4]. The scope of this research is to demonstrate that SERS represents a valuable tool even in case of no chemical interaction between analyte and gold NPs. The first part of the study is dedicated to the synthesis and characterization of different gold NPs in terms of shape, size, plasmon resonance and Raman enhancement efficiency. Then the analytical procedure was set up on a flat surface as model system to standardize SERS methodology for both qualitative and quantitative analysis. Raman mapping was exploited to increase signal reproducibility from spot to spot analysis and to overcome difficulties related to surface inhomogeneity. A sensitive and specific *in situ* detection method of the fungicide on the contaminated surface of an apple was assessed and an accurate method for pyrimethanil quantification on the entire surface of the fruit in accordance with the European law limits was calibrated. The last part of the work is devoted to a real case application and validation.

## 2. MATERIALS AND METHODS

### *2.1 Reagents and materials*

Hydrogen tetrachloroaurate trihydrate (HAuCl4 $3H_2O$ ≥99%), trisodium citrate dihydrate (≥99%), were purchased from Sigma-Aldrich (Milan, Italy).

Sodium hydroxyde (NaOH 97%), Hydrochloric acid (HCl 37%), Nitric acid ($HNO_3$ 68%), absolute ethanol (99.99%), acetone (99,99%) and Hydroxylamine Hydrochloride ($H_3NOxHCl$, 99+%) were obtained by Novachimica (Milano, Italy). SCALA® (400 g/l of Pyrimethanil suspension) was purchased from BASF Italia (Volpiano, Italy). All solutions were prepared with Milli-Q quality water (18 MΩcm). Silicon wafers with a 300 nm of Silicon dioxide layer on top were purchased from Si-Mat (Kaufering, Germany). Apples used for the assays were purchased in a local supermarket in Torino, Italy.

### *2.2 Gold nanoparticles preparation*

All glassware used in the experiment was soaked in aqua regia ($HCl:HNO_3$ 3:1 v/v) and rinsed thoroughly in water and dried with nitrogen prior to use. Spheroidal AuNPs with a diameter of about 30 nm, 40 nm and 55 nm were synthesized according to Frens, 1973 [5]. Briefly, 7 ml, 5 ml and 3.5 ml of a 1% aqueous solution of trisodium citrate were rapidly injected into 500 ml boiling solution of $HAuCl_4$ (0.01% v/v) for the preparation of 30 nm, 40 nm and 55 nm AuNPs, respectively. The mixture was further refluxed for 10 min and then cooled to room temperature under continuous stirring. Larger AuNPs with a diameter of 90 nm and 120 nm were obtained via seed-mediated growth of 30 nm and 40 nm AuNPs, respectively, using an optimized growing procedure based on hydroxylamine hydrochloride [6]. In detail, 4 ml of Au seeds suspension were put into a round-bottom flask with 53.8 ml of Milli-Q water under continuous stirring and the different solutions were added in the following order: 920 µl of 1% v/v aqueous solution of trisodium citrate (stirring for 3 min), 1.4 ml of 10 mM hydroxylamine hydrochloride solution (stirring for 8 min) and 90 µl of 10% w/v $HAuCl_4$ (added dropwise, 1 drop per second). The concentration of 30 nm, 55 nm, 90 nm and 120 nm AuNPs suspensions is 9 $10^{-11}$ mol $l^{-1}$, 6 $10^{-11}$ mol $l^{-1}$, 8 $10^{-12}$, mol $l^{-1}$, 6 $10^{-12}$ mol $l^{-1}$ respectively. The suspensions were kept in continuous stirring overnight at room temperature in the dark before using it.

### *2.3 Gold Nanoparticles Characterization*

AuNPs characterization was done by UV-Vis absorption measurements and by Scanning Electron Microscopy (SEM) imaging. UV-Vis absorption spectra were collected with the Evolution 60s spectrophotometer (Thermo Scientific).

SEM characterization was carried out using a SEM FEI Inspect F in UHV mode with the SE detector. Typical settings for the imaging are: 10 kV accelerating voltage, 2.5 electron beam spot (18 pA) or 3.5 spot (30pA), 10 mm WD. By imaging the particles using SEM, size and shape of AuNPs were characterized as well as the size distribution of the particles. At least 300 nanoparticles were counted for each sample to estimate the mean diameter and the relative standard deviation of the AuNPs.

### *2.4 Preparation for Pyrimethanil standard suspensions and solutions*

Pyrimethanil solubility in water at room temperature is 0.121 g $l^{-1}$; in case of higher concentration it is dispersed in a stable suspension. Pyrimethanil stock standard suspension was prepared by accurately diluting 2 ml of SCALA® (400 g $l^{-1}$ of Pyrimethanil suspension) in 100 ml and 200 ml of Milli-Q water, to reach a concentration of 8 g $l^{-1}$ (8 $10^3$ ppm) and 4 g $l^{-1}$. Pyrimethanil standard solutions were prepared by subsequent dilutions from the stock suspensions in water to reach the following concentrations: 40 mg $l^{-1}$, 30 mg $l^{-1}$, 20 mg $l^{-1}$, 10 mg $l^{-1}$, 5 mg $l^{-1}$ and 1 mg $l^{-1}$. These pure pyrimethanil standards were used for AuNPs aggregation test, SERS efficiency test and to set up the analytical procedure.

### *2.5 AuNPs aggregation test*

Aliquots of pyrimethanil standard suspension (400 mg $l^{-1}$) were mixed in a 1:2 ratio with AuNPs stock suspension. The mixture was shaken with vortex for 3 s and subsequently analysed by UV-Vis in order to monitor the frequency of the plasmon absorption. In these conditions PMT is in high excess with respect to AuNPs and their interaction, if present could not be negligible. Measurements in acidic conditions were performed after adding few drops of 1 M HCl to reach a pH value close to 3. UV-Vis measurements were repeated over four days.

### *2.6 SERS Efficiency Test*

1 µl of a 400 mg $l^{-1}$ pyrimethanil standard suspension was deposited by drop casting on a flat gold surface and let it dry in air for evaporation. 5 depositions were performed on the surface in order to obtain an array of 5 pyrimethanil spots (4 spots for SERS collection and 1 spot for normal Raman reference collection). Four spots were covered with 2 µl of AuNPs and let dry. The PMT spot designed

for reference measurement was covered with 2 µl of water. The concentration of all AuNPs suspension was levelled to have the same exposed surface area (4 $10^{12}$ $nm^2$), avoiding bias in case of larger NPs.

### *2.7 Detection of PMT on pome fruits*

Pome fruit samples such as green apples were bought from a local store. The whole fruit was washed with sodium bicarbonate to remove contaminants from the surface and then spiked with different amount of PMT standard suspensions. In situ detection of pyrimethanil was performed by depositing 2 µl of a 10-fold concentrated 120 nm AuNPs suspension AuNPS suspension on the contaminated peel. Raman mapping collection was performed after the evaporation of the dispersing medium.

The 10-fold concentrated 120 nm AuNPs suspension was obtained by centrifuging the AuNPs stock suspension at 600 g for 12 min and subsequently re-suspending in a proper amount of water.

For an accurate and precise quantification of the fungicide on the entire surface of the fruit, an extraction procedure was carried out by thoroughly rinsing the peel with a known amount of distilled water (usually equal to the fruit weight) to recover pyrimethanil from the surface. Three separated rinses using one third of the total washing volume were performed to increase the extraction efficiency. 2 µl of the resulting solution were deposited by drop casting on a silicon dioxide surface and let them dry in air. 2 µl of a 10-fold concentrated 120 nm AuNPs suspension were then deposited on the PMT spot and analyzed by Raman mapping after drying. The content of PMT in real samples was determined by SERS according to the analytical procedure reported in 2.9.

### *2.8 SERS Measurement*

SERS spectra were recorded using a Thermo Scientific DXR Raman equipped with a microscope, excitation laser source at 780 nm, a motorized microscope stage sample holder, and a charge-coupled device (CCD) detector. Raman equipment is monthly calibrated through a software-controlled calibration tool which ensures wavelength calibration using multiple neon emission lines, laser frequency calibration using multiple polystyrene Raman peaks, intensity calibration using standardized white light sources. The frequency uncertainty is determined by the grating resolution of 5 $cm^{-1}$; the intensity uncertainty was demonstrated to be lower than 5 % using a polystyrene standard. Spectra of samples were collected using a 20x long working distance microscope objective with a 10 mW laser power and a spectral range from 150 to 3400 $cm^{-1}$. The acquisition time was of 5 scans with 1 s exposure time. A Raman map of about 25 spectra was collected on each PMT-AuNPs spot (about 0.5 $mm^2$ area was investigated). From each Raman map one mean spectrum is calculated and used for analysis.

### *2.9 Quantitative calibration and validation of the method*

The instrumental linearity was evaluated from a calibration curve calculated with five levels of PMT concentrations in non-spiked fruit extract, representative of the analysed matrix: 0 mg $kg^{-1}$, 5 mg $kg^{-1}$, 10 mg $kg^{-1}$, 20 mg $kg^{-1}$, 40 mg $kg^{-1}$. 2 µl of each PMT standard solution were deposited by drop casting on a silicon dioxide surface and let them dry in air at room temperature. For the calibration procedure of SERS analysis, 2 µl of a 10-fold concentrated 120 nm AuNPs suspension were deposited on the five spots with increasing concentrations of pyrimethanil. After drying, Raman mapping was performed on each spot, as described in 2.8, and all spectra from each map were averaged for statistical analysis. Each measurement was repeated 4 times to test the measurement repeatability. A Raman band at 2130 $cm^{-1}$ related to AuNPs was exploited to normalize the Raman intensity of pyrimethanil spectrum, minimizing possible variations due to laser power, focal distance, environmental parameters (temperature, humidity) and to overcame variations of the enhancement effect due to the different ratio between the amount AuNPs and analyte molecules. The intensity of PMT Raman band at 997 $cm^{-1}$ was plotted versus pyrimethanil concentration to obtain the calibration curve. The uncertainty of pyrimethanil concentrations was also calculated, as recommended by the GUM [7], in order to meet metrological requirements. Data were fitted by weighted total least square (WTLS) regression by means of a MATLAB®-based tool for calibration problems that is able to deal with uncertainty (and correlation) in both the dependent (average intensities) and independent (concentration) variables. The linearity was estimated by the

reduced chi-square value (χ2). Acceptability criterion to assume the linearity of the response is χ2 close to 1.

Multivariate calibration was performed using Partial Least Square method. PLS regression is based on the maximization of the covariance between variables (spectral frequencies) and response (contaminant concentration) associated to the calibration standards [8]. Six concentrations of pyrimethanil (0 mg $kg^{-1}$, 1 mg $kg^{-1}$, 5 mg $kg^{-1}$, 10 mg $kg^{-1}$, mg $kg^{-1}$, 30 mg $kg^{-1}$, 40 mg $kg^{-1}$) were deposited and covered with AuNPs as described above. For each concentration standard 4 SERS maps were collected and the mean spectra of each map were used as calibration standards. PLS calculation was performed using R based chemometric software. The spectral frequencies considered range from 180 $cm^{-1}$ to 2500 $cm^{-1}$; the range between 500 $cm^{-1}$ and 550 $cm^{-1}$ was excluded so that the peak at 520 $cm^{-1}$ associated to the silicon substrate is not considered during calibration. Only baseline correction was performed before multivariate calculation, the spectra are neither scaled nor centred. The optimal number of PLS components was selected on the basis of the cumulative explained variance (CEV) for each component. An optimization criterion is that CEV is maximized and variables that do not provide further information are excluded. Full cross validation was performed and the minimization of Root Mean Square Error in Cross Validation was considered as an optimization criterion as well.

The validation of both monovariate and multivariate methods was performed using an external sample spiked at low limit contamination (i.e. 7 mg $kg^{-1}$ for apples) and treated as described in 2.7.

## 3. RESULTS AND DISCUSSION

Since the standardization of analytical methods requires well-defined materials with stable and reproducible features, spheroidal AuNPs with different size were fabricated and deeply characterized by SEM and UV-Vis measurements. Figure 1 shows typical SEM images of AuNPs with the mean diameter of 30 nm, 55 nm, 90 nm and 120 nm, respectively. The particle shape was nearly spherical for the nanoparticles of all sizes; the mean diameter and its associated uncertainty are reported in Tab. 1. The surface plasmon resonance peaks of AuNPs suspension were measured to absorb visible radiation at 530 nm, 545 nm, 555 nm and 595 nm for AuNPs dimensions of 30 nm, 55 nm, 90 nm and 120 nm, respectively. As the size of AuNPs increases, the $\lambda_{max}$ of the absorption peak in the UV-vis region was found out to increase from 530 nm to 580 nm, which agrees with the previous consideration that the maximum peak wavelength red-shifts as the relative particle size gets bigger [9].

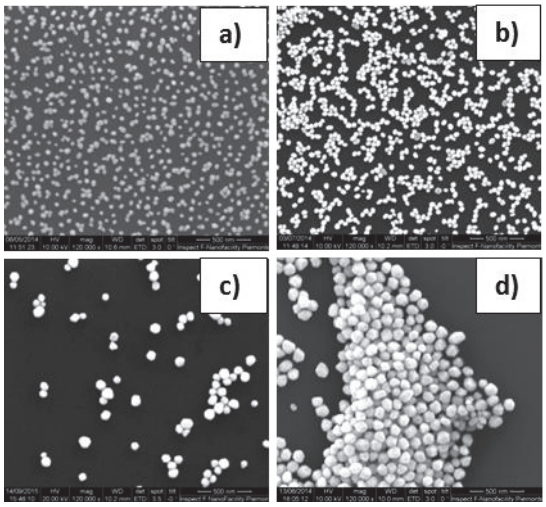


Fig. 1. SEM images of the four examinated AuNPs deposited on a Silicon slide.

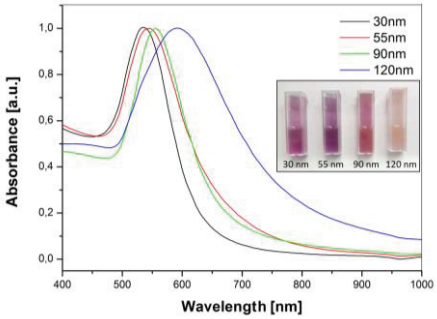


Fig. 2. UV-Vis absorption spectra of AuNPs with the mean diameter of 30, 55, 90 and 120 nm which exhibit an LSPR peak at 530, 545, 555 and 595 nm, respectively.

Several papers already proposed metallic NPs as useful substrates for pesticides detection but in most of these methods a strong chemical interaction between the colloids and the analyte occurred. This binding affinity, normally, induces the aggregation of the metallic NPs and, consequently, a huge enhancement of the Raman signals of the analyte is registered because of the formation of SERS "hot spots" containing the analyte molecules that are bounded to AuNPs. Conversely, the chemical structure of pyrimethanil does not support selective binding with citrate terminated AuNPs and the enhancement of its

Raman signals can be exclusively promoted by the electromagnetic effect, which has to be induced by the proximity of the fungicide molecules and the metallic NPs surface. The chemical interaction of AuNPs with pyrimethanil was studied performing AuNPs aggregation test in suspension by monitoring the LSPR frequency. No shift of the LSPR peaks at higher wavelengths was registered over 15 minutes for the 30 nm, 55 nm, 90 nm and 120 nm AuNPs colloids after adding PMT (400 mg $l^{-1}$), meaning that no AUNPs aggregation is promoted by the analyte since very low chemical affinity exists between AuNPs and the analyte. No shift of the LSPR peaks was further observed after four days, confirming the long term stability of all these colloidal systems in the presence of PMT. Since PMT and AuNPs do not interact in a liquid medium, PMT detection has to be conducted in dry condition in order to promote the absorption of the PMT on the AuNPs surface and to maximize the electromagnetic effect in SERS technique.

The SERS response of four different AuNPs colloids was compared with the aim to select the best enhancing system for our scope (Tab. 1).

Tab. 1. Enhancement factor provided by AuNPs with different size.

| AuNPs diameter [a] (nm) | EF[b] |
|---|---|
| 30±9 | 3.1 ± 0.3 |
| 55±13 | 20.2 ± 1.6 |
| 90±18 | 24.1 ± 1.93 |
| 120±23 | 28.9 ± 2.3 |

[a]Size distribution was calculated statistically by counting the diameter of at least 100 NPs for each type of AuNPs.

All the tested AuNPs were able to enhance the specific peaks of pyrimethanil in SERS analysis compared to the normal Raman spectroscopy. The peak at 997 $cm^{-1}$ was used to compare the intensity of the different AuNPs because it exhibits the highest intensity and it is characteristic of the breathing mode of the PMT aromatic ring [9]. The analytical enhancement factor (EF) for each size of AuNPs was calculated using eq. 1, where $I_{SERS}$ and $I_{NR}$ are the intensity of the vibrational peak in SERS and normal Raman (NR) measurements, respectively, and $C_{NR}$ and $C_{SERS}$ are the concentration of PMT in NR measurements and the SERS measurements, respectively [11].

$$EF = (I_{SERS}\, C_{NR})/(1 + I_{NR} C_{SERS}) \qquad \text{(eq. 1)}$$

The EF increases together with AuNPs size and the highest value is reached when the 120 nm AuNPs are used. It is known that the local electromagnetic enhancement increases with the increasing particle size [11] and as soon as the particles get bigger also the SP band red-shifts, moving closer to the excitation wavelength of the laser (780 nm). This probably explains our observations that the SERS EF generated from AuNPs is maximized when the size of the gold NPs is around 120 nm. Moreover, we can infer that 120 nm AuNPs arrange in a more suitable morphology in terms of roughness and vicinity of NPs on the contaminated surface. Therefore, 120 nm AuNPs were selected and used for the further development of the present methodology.

In order to demonstrate a practical application in the food safety field, green apples were contaminated with PMT trace residues and *in situ* detection of the fungicide on a real sample was initially tested. The surface of a green apple was contaminated by depositing 1 µl of PMT concentrated suspension (40 µg of PMT) on the peel. 0.5 $cm^2$ area was covered approximately in order to create an ultra-contaminated zone on the peel.

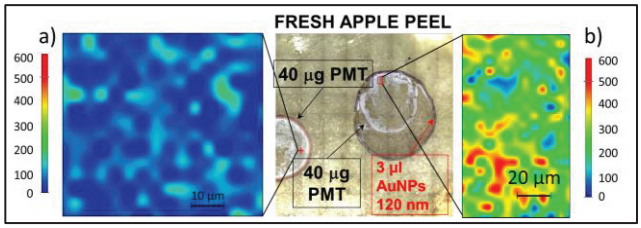


Fig. 4. a) Normal Raman mapping of PMT contaminated region on fresh apple peel; b) SERS mapping of PMT contaminated region on fresh apple peel after deposition of 120 nm AuNPs. The colour scale bar for both a) and b) chemical images is related to the intensity of the PMT peak at 997 $cm^{-1}$.

Raman mapping presented in Figure 4 clearly demonstrated that *in situ* detection of PMT on the apple peel only occurs when AuNPs are applied on the surface, while very low or no PMT signals were registered in the contaminated regions in absence of AuNPs, meaning that normal Raman technique is not sensitive enough to detect low amounts of PMT on the surface. The signal to noise ratio (S/N) increases from S/N = 1.2 for NR to S/N = 5 for SERS measurements. Therefore, this approach could be easily used to achieve *in situ* detection of PMT and to discriminate the type of fungicide/pesticide on

the fruit surface based on the specificity of the Raman fingerprint.

However, this methodology would not be reliable enough to provide a quantitative information on the entire surface of the apple due to fact that only a small portion of the surface is analysed and the colloids tend to randomly aggregate on inhomogeneous surfaces, such as fruits' peel, leading to a lack of reproducibility when spot-to-spot tests are conducted and when different fruit specimen are compared. In order to develop a quantitative methodology, an external calibration method was on a flat model surface was then preferred.

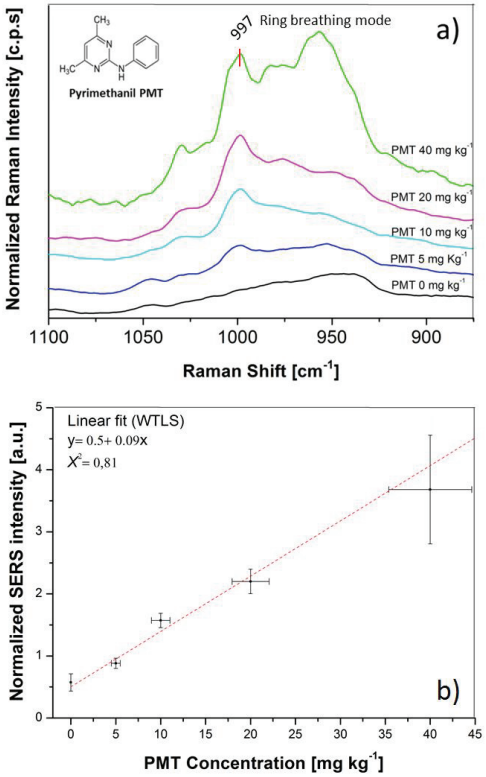


Fig. 5. a) Normalized SERS spectra of 120 nm AuNPs with 5 levels of PMT standard in negative matrix pool (representative of the analyzed matrix): 0, 5, 10, 20 and 40 mg $kg^{-1}$; b) Linear calibration curves obtained by WTLS regression.

Five concentrations of pyrimethanil (0, 5, 10, 20, 40 mg $kg^{-1}$) were deposited by drop casting on a silicon dioxide surface and covered with 120 nm AuNPs. An average spectrum of each SERS map was calculated and normalized to the AuNPs peak at 2130 $cm^{-1}$, which was considered as internal reference to eliminate the effects of the matrix and the enhancement effect due to the different ratio between the amount of AuNPs and analyte at each standard concentration (Fig. 5a). Normalized SERS intensities at 997 $cm^{-1}$ were plotted as a function of PMT concentration and a WTLS regression was used for fitting the data of PMT concentrations and Raman intensities taking into account their associated variance (Fig. 5b). The uncertainty associated with the concentration values was calculated by combining together, the different sources of uncertainties which affect the solution concentration (B-type contributions due to the purity of the PMT and the volume measurement). The standard uncertainty associated with y values was calculated as A-Type uncertainty on the basis of the standard deviation of the intensities at 997 $cm^{-1}$ within each Raman map. The forcefulness of the fit was confirmed by the reduced chi-square value which is attested at 0.8.

However, even if the WTLS regression provided good linearity as demonstrated by low $\chi 2$ value, the calculated uncertainty for slope and intercept are not negligible and they might affect the reliable quantification of PMT on real samples and method resolution. Therefore, it was decided to test a multivariate approach in order to minimize the random variability associated to a single variable and to consider simultaneously the whole information contained in spectral data. A new calibration method was set up using PLS regression to increase the method stability. PLS plots are shown in Figure 6.

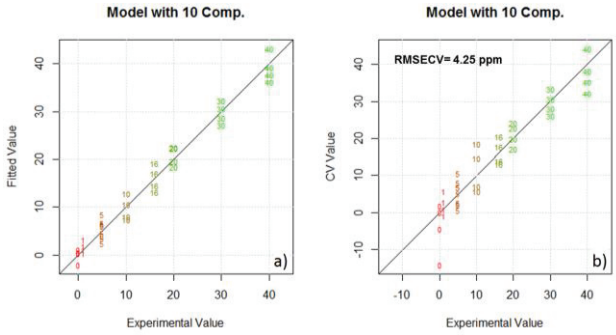


Fig. 6. PLS calibration PLOTS a) plot of fitted value corresponding to calibration standards versus the true values; b) full cross validation values versus true values.

The optimized method provides an RMSECV (root mean square error in cross validation) of 4.25 and cumulative explained variance of 89.11 % when 10 PLS components are considered. The plot of fitted values versus true values (Fig. 6 a) demonstrates a good correlation between spectral data and known responses, as confirmed by full cross validation test (Fig. 6 b).

In order to compare the real applicability of the two proposed methods, an external validation test was performed green apples green apples spiked with PMT at 7 mg $kg^{-1}$. The contaminant was recovered from the apple peal following an optimized washing procedure and the extracted PMT solution was then analysed. A contamination level of 8.65 ± 4.09 mg $kg^{-1}$ and 6.89 ± 3.06 mg $kg^{-1}$ 397 was calculated using the calibration procedures based on WTLS and PLS, respectively. Both values were in agreement with the spiked amount of PMT (7 mg $kg^{-1}$) on the apple, demonstrating the applicability of both methodologies on real samples. However, the mean percentage error (MPE) calculated over 5 repeated measurements was 32.8 % for the monovariate calibration and 18.7 % for the PLS. These results confirm that PLS methodology provides higher accuracy and intra-day repeatability than monovariate analysis and it is more suitable for PMT detection on pome fruits within the European legislation limits.

## 4. CONCLUSIONS

A sensitive and rapid method to detect and quantify residues of pyrimethanil on pome fruits was developed using AuNPs and Raman spectroscopy. Spheroidal AuNPs with different size were synthetized and tested to determine the highest enhancement factor (EF) in pyrimethanil detection. A Raman mapping strategy was exploited to increase signal reproducibility from spot to spot analysis and to minimize bias due to different local surface morphologies. The optimized methodology was tested on real samples providing: i) sensitive and specific *in situ* detection of the fungicide on the contaminated fruit surface; ii) a metrological tool for pyrimethanil quantification on the entire surface of pome fruits in accordance with the European law limits. The analytical procedure was set up on a silicon dioxide flat surface, as a model system, to standardize SERS methodology for quantitative analysis. The method here developed is sensitive and fast; it can be applied in routine analysis for pyrimethanil residue detection on apples and has the potential for broad applications in analyses of other hazardous chemicals in food.

## ACKNOWLEDGEMENTS

The present work has been supported by EMRP project " Q-AIMDS". EMRP in jointly founded by EMRP participating countries within EURAMET and the European Union.
Part of this work was carried out by NanoFacility Piemonte, INRiM, a laboratory supported by Compagnia di San Paolo (Italy).

## REFERENCES

[1]S. Schlücker, Angew. Chem. Int. Ed., 2014, 53, 4756-4795.
[2]Jeanmaire, D. L.; van Duyne, R. P.; Journal of Electroanalytical Chemistry; 84 (1977) 1–20.
[3]Ruyan Hou, Shintaro Pang and Lili He; Ananlytical Methods (2015) DOI: 10.1039/c5ay01058f
[4] Review of the existing maximum residue levels (MRLs) for pyrimethanil according to Article 12 of Regulation (EC) No 396/2005, EFSA Journal 2011;9(11):2454
[5]Frens, G. (1973). Controlled Nucleation for the Regulation of the Particle Size in Monodisperse Gold Suspensions. Nature Physical Science 241:20-22.
[6] Li JF, Tian XD, Li SB, Anema JR, Yang ZL, Ding Y, Wu YF, Zeng YM, Chen QZ, Ren B, Wang ZL, Tian ZQ (2013) Surface analysis using shell-isolated nanoparticle-enhanced Raman spectroscopy. Nature Protocols 8 (1):52-65.
[7] Evaluation of measurement data – guide to the expression of uncertainty in measurement, JCGM 100:2008 (GUM 1995 with minor corrections). file:///C:/Users/Ufficio/Downloads/JCGM_100_2008_E.pdf
[8] Wold, H., Partial Least Squares. Encyclopedia of Statistical Sciences, doi:10.1002/0471667196.ess1914.pub2
[9]Hong S, Li X (2013) Optimal Size of Gold Nanoparticles for Surface-Enhanced Raman Spectroscopy under Different Conditions. Journal of Nanomaterials http://dx.doi.org/10.1155/2013/790323.
[10]Herzberg G (1988) Citation Classic - Molecular-Spectra and Molecular-Structure .2. Infrared and Raman-Spectra of Polyatomic-Molecules. CC/Eng Tech Appl Scis (13):16-16.
[11]Kelly KL, Coronado E, Zhao LL, Schatz GC (2003). The optical properties of metal nanoparticles: The influence of size, shape, and dielectric environment. Journal of Physical Chemistry B 107 (3):668-677.